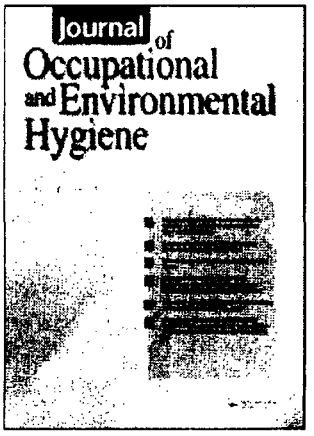

Journal of Occupational and Environmental Hygiene
Publication details, including instructions for authors and subscription information:
http://www.informaworld.com/smpp/title~content=t713657996

Performance of Membrane Filters Used for TEM Analysis of Asbestos

First Published on: 01 October 2007
To cite this Article: Webber, James S., Czuhanich, Alex G. and Carhart, Laurie J. (2007) 'Performance of Membrane Filters Used for TEM Analysis of Asbestos', Journal of Occupational and Environmental Hygiene, 4:10, 780 - 789
To link to this article: DOI: 10.1080/15459620701588385
URL: http://dx.doi.org/10.1080/15459620701588385

Journal of Occupational and Environmental Hygiene, 4: 780–789
ISSN: 1545-9624 print / 1545-9632 online

DOI: 10.1080/15459620701588385

Performance of Membrane Filters Used for TEM Analysis of Asbestos

James S. Webber, Alex G. Czuhanich, and Laurie J. Carhart

Wadsworth Center, New York State Department of Health, Albany, New York

This article presents findings related to characteristics of membrane filters that can affect the recovery of asbestos and the quality of preparations for transmission electron microscopy (TEM) analysis. Certain applications and preparation steps can lead to unacceptable performance of membrane filters used in analysis of asbestos by TEM. Unless substantial care is used in the collapsing of mixed-cellulose ester (MCE) filters with an acetone hot block, grid preparations can suffer and fiber recoveries can be compromised. Calibration of the etching depth of MCE filters, especially at differing locations in an asher's chamber, is critical for reliable fiber recovery. Excessive etching of MCE filters with aerosol-deposited asbestos can lead to loss of short fibers, while insufficient etching of MCE filters with aqueous-deposited asbestos can, paradoxically, also lead to loss of short fibers. Interlaboratory precision on MCE filters is improved by aerosol-deposited asbestos, as opposed to aqueous deposition. In comparison, straightforward preparation, improved solvents, and reduced contamination make PC filters an increasingly acceptable alternative. Variations in the geometric configuration during application of carbon films can lead to fiber loss and unacceptable grid quality for either type of filter.

Keywords asbestos, membrane filter, mixed-cellulose ester (MCE) filter, polycarbonate (PC) filter, transmission electron microscopy (TEM)

Address correspondence to: James S. Webber, Wadsworth Center, PO Box 509, Albany, NY 12201; e-mail: webber@wadsworth.org.

INTRODUCTION

Analysis of asbestos in the environment is performed with microscopes. The thinnest asbestos fibers, as narrow as 0.02 μm, can be detected only by electron microscopes because light microscopy's resolution is typically 0.2 μm. Transmission electron microscopy (TEM) also allows identification of crystalline structure through electron diffraction and determination of chemical composition if equipped with an energy-dispersive X-ray detector. Two types of membrane filters are used for collection and TEM analysis of asbestos in the environment. Mixed-cellulose ester (MCE) filters rely on filtration throughout their depth to collect most particles larger than a nominal size. Long fibers are easily trapped on the surface, while shorter fibers can penetrate more deeply into the matrix. Chatfield[1] provides a good discussion of this process.

Polycarbonate (PC) filters, on the other hand, are featureless films with uniform-diameter pores that collect particles on a flat surface. Figure 1 shows these surfaces, as imaged by scanning electron microscopy (SEM) on a LEO 1550vp Field Emission Gun Scanning Electron Microscope (Carl Zeiss, Inc., Peabody, Mass.).

ISO 10312 and all ASTM methods (D5755, D5756, D6281, and D6480) for analysis of asbestos in air and dust permit use of either filter type.[2,3] Likewise, MCE and PC filters are both acceptable to the U.S. Environmental Protection Agency (EPA) for sampling air and water. Although PC filters are acceptable under the Asbestos Hazard Emergency Response Act of 1986 (AHERA) guidelines,[4] the senior author has never observed them used by any of the more than 120 different TEM laboratories that he has assessed since 1988, including 65 of the remaining 79 TEM laboratories certified for AHERA analysis at the end of 2006.

Whereas PC filters were the only medium allowed for testing of potable water under EPA Method 100.1,[5] the introduction of EPA Method 100.2 in 1994 allowed the use of MCE filters as well.[6] Many TEM laboratories, comfortable with and efficient in the use of MCE filters for AHERA analysis, have switched to MCE filters for water filtration. The National Institute for Occupational Safety and Health (NIOSH) allows only MCE filters for sampling asbestos fibers from the air.[7]

This article presents findings related to characteristics of membrane filters that can affect the recovery of asbestos and the quality of preparations for TEM analysis. Some of these findings arose from investigations within our own laboratory, characteristics or conditions of TEM grids or results received in proficiency testing (PT) rounds, and observations made at laboratories during on-site assessments.

MCE Filters

MCE filters, because of their tortuous surface, require more preparation steps than PC filters. A carbon film applied directly to the surface of an MCE filter (Figure 1, panels b and c) would be unsuitable for TEM analysis for several reasons: wrinkling and overlapping of the applied carbon film would result from

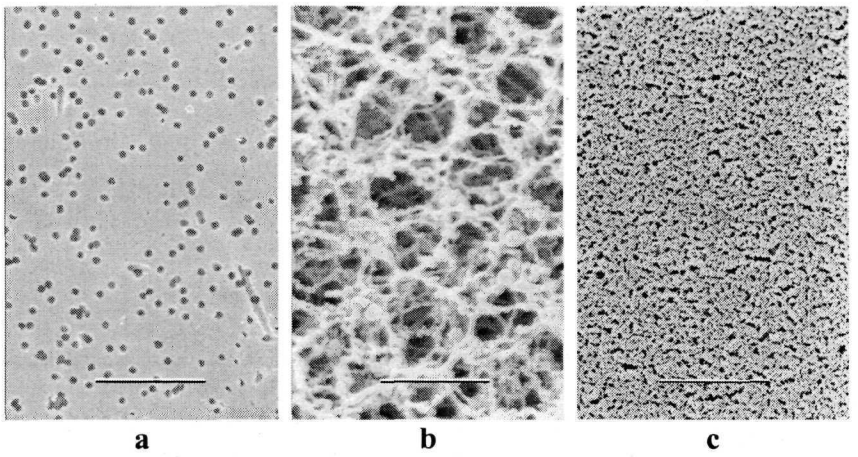

FIGURE 1. Scanning electron micrographs of membrane filters. Scale bar length is 5 μm. (a) 0.4-μm PC filter; (b) 0.45-μm MCE filter; (c) 0.1-μm MCE filter.

the cavernous undulations of the surface, gaps would be left because of surface irregularities, and fibers trapped in spaces below the filter surface would not be captured in the applied carbon film.

In a seminal work, Burdett and Rood[8] developed a technique for MCE filters that incorporated a collapsing step that brought trapped fibers closer to a now-smooth surface, and a plasma-etching step that uncovered embedded fibers. This process is illustrated in Figure 2, where the fibers are depicted being collected on the filter surface in the upper left corner. A section of filter is placed fiber-side up on a glass slide, the filter is collapsed in solvent, the collapsed surface is etched to expose any fibers below the smooth surface, the surface is carbon coated to trap exposed fibers, and remaining filter material is removed when placed on a TEM grid in solvent. Ideally, all asbestos fibers collected on MCE filters will be captured in the applied carbon film for viewing, as shown in the left-hand drawing of the middle row. In practice, however, either insufficient etching or excessive etching can lead to fiber loss, as depicted in the bottom row of Figure 2.

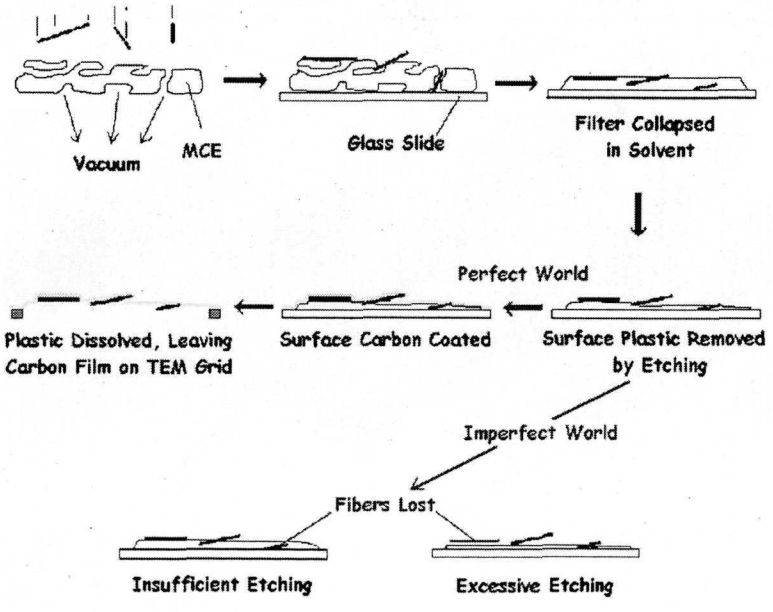

FIGURE 2. Procedure for preparing MCE filters for TEM analysis. The etching step would not be applied for NIOSH 7402 preparations.

Collapsing MCE Filters

Today, MCE filters are usually collapsed by one of three methods. The original method of Burdett and Rood[8] employed a solution of 35% dimethylformamide (DMF) onto which an MCE wedge was placed and allowed to clear for 15 min on a warm surface. In the AHERA method, [4] the MCE wedge is affixed to a slide and placed into a petri dish containing an acetone atmosphere (AA) for several minutes. Finally, a hot block (HB) technique, introduced for clearing MCE filters for phase-contrast light microscopical (PCM) counting of fibers, is now seeing wide application for TEM because it rapidly collapses an MCE filter wedge—a few seconds vs. several minutes for other methods.[9]

We surveyed TEM laboratories that had participated in the New York State Department of Health Environmental Laboratory Approval Program (ELAP) proficiency testing (PT) rounds between 2000 and 2006 to determine which collapsing methods they had used for MCE filters. We compared possible relationships between these reported collapsing methods and quantitative results these laboratories had reported for PT samples. Individual laboratory results (structures/mm^2) for each PT sample were divided by the PT consensus mean for that sample. Perfect agreement of a laboratory's result with the consensus mean, then, would yield 100% recovery. We limited evaluation to those laboratories that had reported results for at least 80% of the aerosol-generated AHERA PT samples (21 amphibole samples and 6 chrysotile samples) distributed during that period.

To eliminate laboratories that were inconsistent in their quantitation, we restricted evaluation to laboratories whose recoveries for each of the two fiber categories yielded relative standard deviations (RSD) less than 40%. For filters with amphibole asbestos, there was essentially no difference in mean recoveries (97% to 120%) among the three collapsing methods (Table I). Chrysotile, on the other hand, was strikingly affected, with DMF (155%) producing almost twice the recovery of the HB (87%). Large interlaboratory variation prevented detection of statistical significance, however.

TABLE I. Relationship of MCE-Collapsing Method to Fiber Recovery in Aerosol-Generated ELAP PT Samples

Asbestos Type	Collapsing Method	Number of Labs	Mean Recovery (%)	RSD (%)
Amphibole	DMF	5	120	18
	AA	4	100	8
	HB	13	97	12
Chrysotile	DMF	5	155	26
	AA	4	123	15
	HB	9	87	18

Notes: DMF = dimethylformamide; AA = acetone atmosphere; HB = hot block; RSD = relative standard deviation.

We compared HB and DMF collapse effects using a 0.45-μm MCE filter from an ELAP PT round (29 participating laboratories, collapsing techniques not reported) that had produced a consensus mean of 727 (standard deviation [SD] = 215) fibers/mm^2. Our DMF-prepared grids produced 806 (SD = 304) fibers/mm^2, which was slightly more than the 757 (SD = 258) fibers/mm^2 from our HB-prepared grids, but the large standard deviations precluded statistical significance. Fiber-length distributions from the two preparation methods

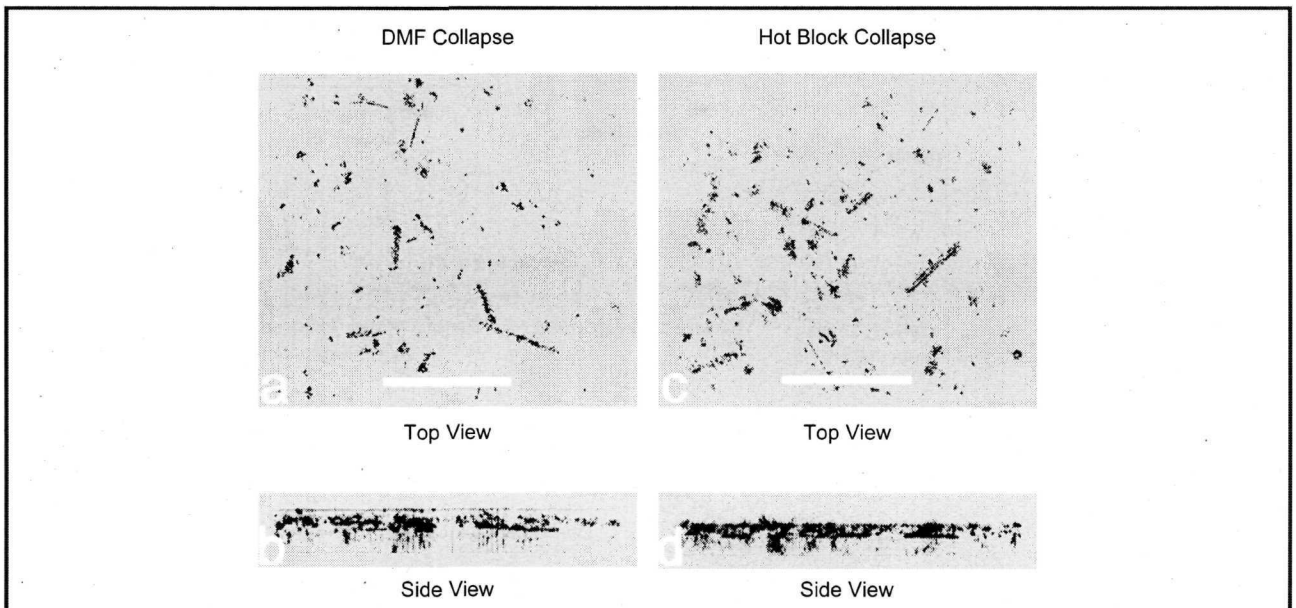

FIGURE 3. Confocal micrographs top and side views of sections of a single 0.45-μm MCE filter prepared using DMF (a and b) and HB (c and d) Scale bars, 125 μm, apply to all images.

were identical. The lack of statistical difference in our intra-laboratory comparison might not reflect the results of current practices in other laboratories, in that our use of the HB was carefully controlled to prevent excessive hot-vapor forces and flooding (discussed later).

Movement of Fibers During Collapse

Burdett and co-authors[10] used confocal light microscopy (CFLM) to determine the configuration of collected asbestos fibers within the depths of an MCE filter. We adapted CFLM to evaluate fiber distribution through the filter depth as a function of the collapsing method used. For our study, an aerosol-generated suspension (aerosol generator discussed later) of milled amosite was collected at 1 L/min on 0.45-μm MCE filters loaded in standard 25-mm cassettes. Two wedges from a single filter were collapsed on separate glass slides, one by HB and the other by DMF. These were examined by CFLM, with an area approximately 350 μm on a side analyzed over the complete depth of the collapsed filter. The top view of the DMF-collapsed filter is shown in Figure 3, panel a. Resolution is insufficient to show most fibers, but a few large ones are visible. The smaller fibers appear in amorphous clumps.

When the DMF-collapsed filter area is viewed from the side (CFLM compresses the entire ~350-μm width into this view), the top surface of the collapsed filter is visible as a straight horizontal line, with the bottom surface the fainter horizontal line about 40 μm below that (Figure 3, panel b). Most of the fibers are located about 10–20 μm below the surface. The HB-collapsed section is slightly thinner, about 35 μm thick (Figure 3, panel d). This section seems to lack the original overlying filter material of the DMF-collapsed section, i.e., the straight horizontal line above the fibers visible in Figure 3, panel b.

Instead, this filter surface has eroded during the hot acetone's vigorous interaction. This leaves HB-prepared fibers more exposed, increasing the likelihood that the subsequent etching step (discussed in a later section) might be more likely to erode all attachment points for the topmost fibers. These detached fibers could be lost between etching and carbon-coating steps. Again, our use of HB was carefully controlled; erosion of surface materials may be more substantial where HB application is more vigorous.

Even more problematic is the movement of fibers along the filter surface during HB collapse. The authors, in observing application of the HB method during many laboratory assessments, noted that the heated acetone vapor was frequently generated with such vigor that waves of hot acetone would ripple outward from the wedge's center, flooding the surrounding slide. Subsequently, we duplicated this HB practice by introducing acetone at a faster-than-normal rate, causing it to overflow a filter wedge. This wedge was from a filter with an intentional aerosol-generated overloading (~10,000 fibers/mm^2) of amosite to easily portray fiber distribution. A second wedge from the same filter was collapsed by DMF solution.

Scanning electron micrographs of these filter surfaces (Figure 4) show that fibers remain uniformly distributed in their aerosol-deposited positions after DMF collapse (panel a), whereas fibers have been washed into windrows by HB's vigorous lateral forces (panel b). Scanning along the edges of the HB-prepared wedge with SEM did not reveal a substantial number of fibers, so actual loss of fibers from the filter surface itself appeared unlikely during the preparation.

This redistribution of fibers by HB creates severe analytical difficulties. The first is that TEM analysis is limited to a very small area of the filter. This is illustrated (Figure 4, panel c) where a typical TEM grid with 0.01-mm^2 openings is superimposed over a negative image of panel b. Here, fiber concentrations in different grid openings vary by more than an order of magnitude, yielding enormous standard deviations as multiple grid openings are analyzed separately. This portends poor statistical reconstruction of original fiber concentrations for AHERA analyses, where analysis is typically limited to five grid openings, or about 0.05 mm^2. (This is less of a problem for the PCM method for which HB was developed—100 fields of ~0.008 mm^2 [~0.8 mm^{2}total] are analyzed across a much broader area, increasing the likelihood of representative counting.)

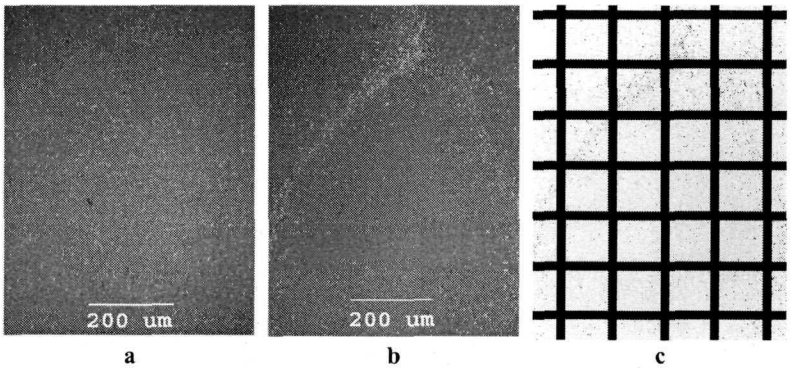

FIGURE 4. Scanning electron micrographs of sections of a single 0.45-μm MCE filter with aerosol-deposited amosite prepared by (a) DMF, (b) HB, and (c) same image as b but negative with superimposed TEM grid with 100-μm openings

The second problem with uneven distribution is a possible unconscious partiality by an analyst to select the cleaner grid openings for analysis, thus producing erroneously low fiber concentrations. This can be somewhat ameliorated by using a protocol that dictates *a priori* which grid openings are to be counted. This can be a pre-set pattern employed for all grids or a program that generates a list of random grid openings.[11]

The final problem is that when particles are piled up, as in the HB windrows, the evaporated carbon (discussed later) will have gaps that lead to breakage of the film. Grid openings with these broken films will not be analyzed, again leading to a negative bias in results.

Tilting Fibers During Collapse

Burdett et al.[10] also used CFLM to evaluate the tendency of collected fibers to be tilted within uncollapsed MCE filters.Their work indicated that most fibers were within ±25° of horizontal, with out-of-plane angle decreasing with increasing fiber length. Because they predicted that collapsing would remove most tilt, we used TEM to investigate fiber tilt in collapsed filters. (Our CFLM was not used because of its inability to resolve thin fibers.) We selected only fibers that were oriented on the grid with their lengths perpendicular (±10) to the tilt axis of the TEM goniometer. These were tilted to determine the tilt angle producing the greatest fiber length on the viewing screen.

After performing this exercise on several filter types (Table II, it became apparent that the greatest proportion of tilted fibers were collected on larger pore MCE filters. The large textural irregularities on 0.45-μm MCE surfaces (Figure 1, panel b) allow shorter fibers to penetrate at an angle vs. the smoother 0.1-μm MCE surfaces (Figure 1, panel c), and collapsing did not completely bring these fibers to horizontal.

To determine if collapsing method affected tilt, we prepared a single crocidolite-deposited 0.45-μm MCE filter using several methods. One wedge was collapsed by exposure to a warm acetone atmosphere in a sealed petri dish. Another wedge was collapsed in DMF solution. Two more wedges were collapsed using HB, one with the slide at room temperature and the other with a slide prechilled to 0°C. As seen in Table III, use of HB with a slide at room temperature produced the largest average fiber tilt (3.9°) and largest percentage (19%) of fibers exceeding 10 tilt. This might result from the very short liquid phase produced by HB at room temperature and subsequent inability of surface tension to draw fibers to a horizontal position.

Finally, we evaluated the effect of fiber length on fiber tilt. Table IV reveals that shorter fibers were most likely to be tilted. This is expected, since longer fibers are more apt to straddle the high points of textured surfaces of 0.45-μm MCE filters (Figure 1, panel b) to lie flat, in the same way that smaller pore filters are more likely to minimize tilting of shorter fibers. This is consistent with Burdett's[10] CLFM study of fiber orientation in uncollapsed MCE filters. However, Burdett predicted that most tilt would be removed by collapsing and "any bias due to foreshortening effects are likely to be minimal." [10,p.221] Our results indicate otherwise, that some short fibers remain tilted after collapsing.

Because HB is not typically used with chilled slides, conventional use of HB may be producing false negatives for reasons of length and SAED criteria. Fibers barely long enough to meet measurement criteria may be tilted sufficiently to appear shorter than the cut-off and therefore eliminated from counts. For example, a 0.6-μm fiber tilted at 34° would appear shorter than 0.5 μm and would not be counted under AHERA rules. As previously discussed (Table IV), short fibers are indeed the most likely to be tilted in collapsed MCE filters. Undercounting of short fibers becomes increasingly important in light of the recent review that demonstrated that short fibers are medically relevant.[12]

The second analytical problem with tilted fibers, regardless of length, is that SAED layer-line spacings will move farther apart on the screen as fiber tilt increases. Our tilting investigations have revealed that a fiber tilted at 20° or more will yield layer-line spacings that deviate more than 10% from 0.53 nm. This would disqualify the fiber from meeting SAED criteria for asbestos' silicate spacings.

TABLE II. Fiber Deviations from Horizontal on Carbon Films

Filter Type	0.1 PC	0.1 MCE	0.22 MCE	0.45 MCE
Fibers measured	30	32	76	203
Mean tilt (degrees)	0.5	0.16	1.44	2.36

Note: MCE = mixed-cellulose ester; PC-polycarbonate.

TABLE III. Effect of MCE-Collapsing Method on Fiber Tilt

Collapsing Method	AA	DMF	HB Cold	HB Warm
Fibers measured	34	41	37	31
Mean tilt (degrees)	2.1	1.3	1.2	3.9
% Fibers tilted > 10°	15	7.3	10	19

Note: MCE = mixed-cellulose ester.

TABLE IV. Effect of Fiber Length on Probability of Tilting

	Fiber-Length Range (μm)		
	0.5–2	2–5	>5
Fibers measured	57	64	22
Mean tilt (degrees)	3.1	1.8	0.0
% Fibers tilted > 10°	11	6	0

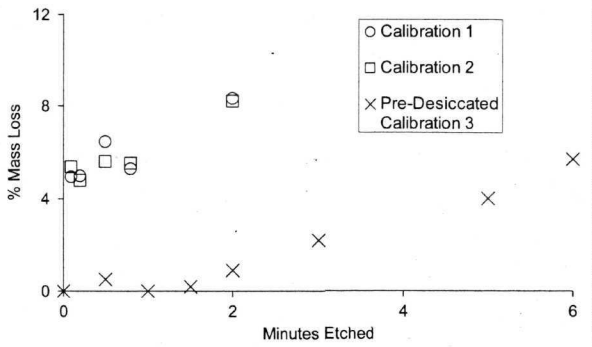

FIGURE 5. Mass loss of 0.45-μm MCE filter during etching, with and without compensation for desiccation

Shrinkage and Warping During Collapse

Chatfield[1] warns that the area of an MCE wedge shrinks during collapse. We collapsed whole 0.1, 0.22, 0.45, and 0.8-μm, 25-mm MCE filters using both HB and DMF and found shrinkage to average 3% for HB and 6% for DMF. This, of course, will create a marginal positive bias in calculated fiber concentrations. As cautioned by the authors when introducing this direct-transfer MCE technique, care must be taken to use only enough solution to soak the entire wedge.[8] Excess DMF can cause the filter area to increase as the dissolving filter moves outward to fill the area of the DMF puddle, whereas insufficient DMF will not clear the entire filter and may cause shrinkage. We have determined that 20 μL DMF solution will properly saturate a quarter wedge of a standard 25-mm, 0.45-μm MCE filter.

Laboratories that wish to avoid use of the HB or DMF can utilize acetone in a closed petri dish or similar chamber. Collapsing times can be substantially reduced by increasing the temperature, as shown in Table V. We determined the mass/area of different pore size MCE filters but found that the rate of collapse had no consistent relationship between either the mass/area or pore size. Wedges can be taped to the slide to prevent potential curling and minimize any shrinkage.

TABLE V. Collapsing Time of Different Pore-Size MCE Filters in Static Acetone Atmosphere as a Function of Temperature

MCE Pore Size (μm)	Mass (mg/cm^2)	Seconds to Clearing 25°C	Seconds to Clearing 50°C
0.1	6.54	88	43
0.22	7.14	80	36
0.45	6.65	77	37
0.8	5.98	104	47

Notes: MCE = mixed-cellulose ester. Static acetone atmosphere in closed petri dish.

Etching MCE Filters

Fibers that are completely below the surface of the collapsed filter are beyond the reach of the applied carbon film and will likely be washed away during final dissolution of the filter material. The EPA's AHERA method requires that "a 1–2 μm (10 percent) layer of collapsed surface will be removed" [4,p.41881] by plasma etching to expose any such buried fibers. A widely used calibration method is to etch a tared collapsed filter for measured time intervals to determine the duration needed for a target percentage, e.g., 10% mass removal.

We found that our regression lines for best-fit of time vs. percentage of etching seldom passed through the expected x-y origin (Calibrations 1 and 2 in Figure 5). Desiccation of the collapsed filter during initial vacuum conditions in the etcher was identified as the cause of this nonetching loss. That is, even without plasma etching, the collapsed filter lost about 5% of its mass (as water) after exposure to the vacuum of the etcher chamber. If we allowed the collapsed filter to desiccate for 5 min in the etcher and then immediately tared it, etching calibration regressions would pass through the x-y intercept, as seen for Calibration 3.

To save time, laboratories will place several filter wedges in an etcher chamber for simultaneous etching. Many of these laboratories, however, have not determined the effect that wedge placement within a chamber's geometry has on etching rates. We placed 12 filter wedges (four rows from front to back, by three rows from side to side) in our etcher (LFE 104 Barrel Plasma System) for simultaneous etching. We found that etching of wedges in the front two rows (Rows S4 and S3 in Figure 6) was 50% greater than for wedges in the rear of the chamber (Row S1).

Another in-laboratory investigation verified a finding by Chatfield[1] that etching depth substantially affects fiber recovery. We divided into six wedges a single 0.45-μm MCE filter on which an aqueous suspension of chrysotile had been collected. One each of five wedges was etched for times equivalent to 1%,

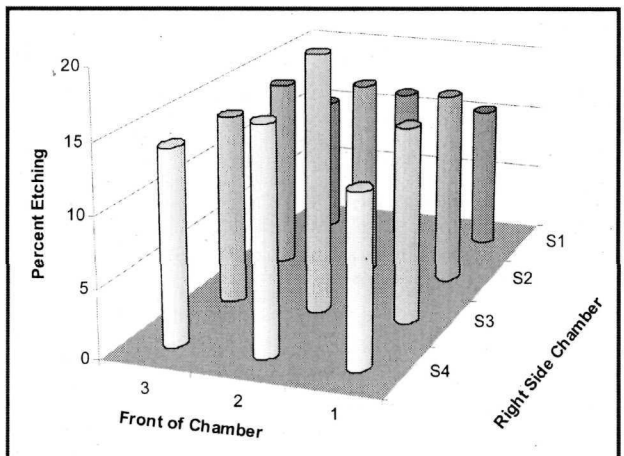

FIGURE 6. Effect of placement of filter wedges within etcher chamber on etching rate

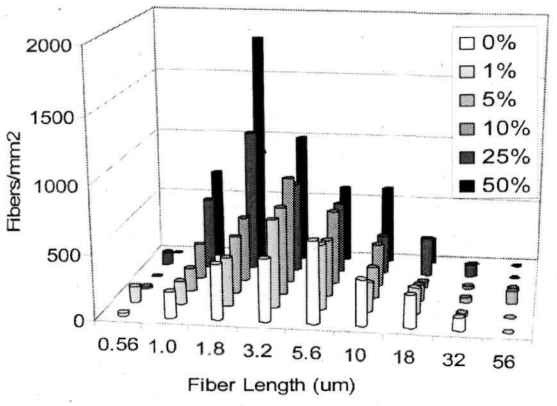

FIGURE 7. Fiber-length distributions relative to etching percentage, for six wedges prepared from a single 0.45-μm MCE filter with aqueous-deposited asbestos

5%, 10%, 25%, and 50% mass removal. The sixth wedge was not etched. All sections were carbon coated and prepared on TEM grids for analysis. Figure 7 reveals substantial differences in fiber recovery linked to etching. Short ($\leq$3.2 μm) fibers were not fully recovered until etching far exceeded 10%. These short fibers were obviously carried by hydraulic forces deep into the tortuous MCE matrix.

The same trial was conducted with a 0.1-μm MCE filter. Although short fibers were moderately reduced at low etching percentages (Figure 8), the trend was not as pronounced as it was for the 0.45-μm MCE filters. This indicates that smaller pore MCE filters may be more acceptable for filtration of water samples, which is consistent with the less torturous surface of the smaller pore filter seen in Figure 1.

Finally, we ran a 0.45-μm MCE filter containing aerosol-deposited asbestos (aerosol generator is described later)

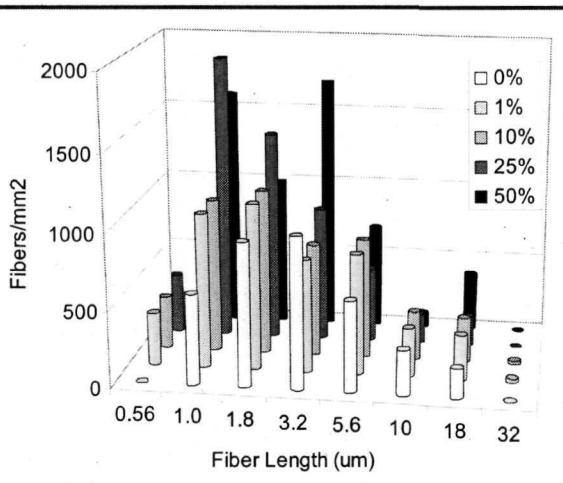

FIGURE 8. Fiber-length distributions relative to etching percentage, for six wedges prepared from a single 0.1-μm MCE filter with aqueous-deposited asbestos

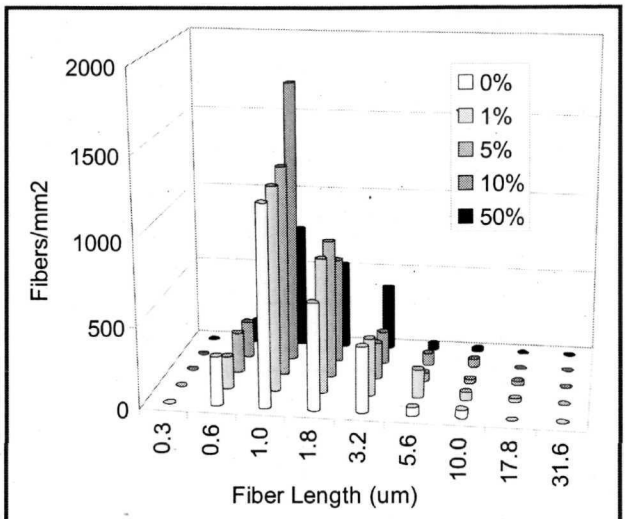

FIGURE 9. Fiber-length distributions relative to etching percentage, for six wedges prepared from a single 0.45-μm MCE filter with aerosol-deposited asbestos

through the same regimen. Interestingly, etching rate also affected short-fiber recovery for aerosol-deposited asbestos but in the opposite manner. As seen in Figure 9, a filter wedge processed with 50% etching yielded fewer short fibers than wedges receiving less etching. This difference was significant ($p < 0.05$) for fiber lengths shorter than 1.8 μm.

This short-fiber loss at 50% etching was probably due to the tendency for airborne fibers to be collected on the filter surface rather than being forced deeply into the filter depth (as are waterborne fibers). Short fibers will have less surface area in contact with the collapsed filter than will long fibers, and this reduced contact area would be more quickly eroded by the plasma, causing more frequent detachment. This potential loss of surface fibers also bodes poorly for MCE filters prepared by HB, given our earlier finding that fibers tend to accumulate atop the surface when HB is used. Note that NIOSH 7402 Method[7] does not employ etching because this will remove organic fibers, which are a target of identification. Fortunately, this method counts only fibers longer than 5 μm, which, on the basis of the above results, are not affected by etching.

Regardless of the extent of fiber recovery, excessive etching interferes with analysis, as shown in the paired electron micrographs of DMF-collapsed 0.45-μm MCE filters in Figure 10 (imaged with a Hitachi H7100 Scanning Transmission Electron Microscope; Tokyo, Japan, at a nominal magnification of 20,000×). At 0% etching, the filter surface is flat and featureless with the fiber (easily visible in the TEM micrograph) barely touching the surface (SEM micrograph) and only just captured by the carbon film.

As etching increases, larger and deeper sections are eroded from the filter surface. Even by 10%, the surface of the filter has achieved sufficient texture to become noisy to the analyst's eye. From this point on, etching artifacts can tire the analyst, thereby hindering detection of thin or short asbestos fibrils and

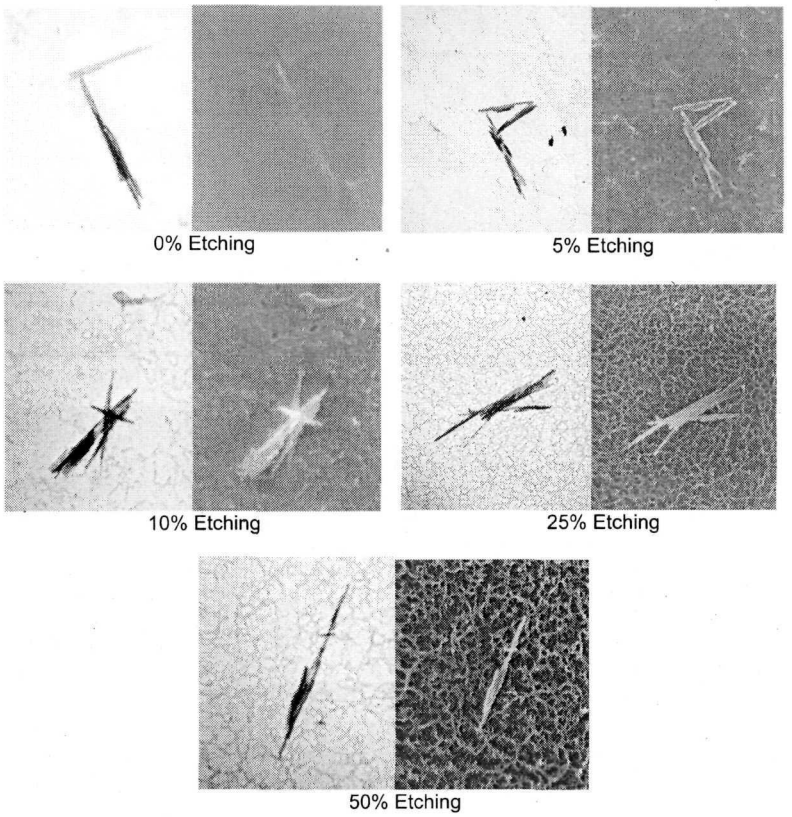

FIGURE 10. Effects of etching on MCE filter surfaces. The dark fibers against a light background (left side of each pair) is a TEM micrograph while the accompanying light fibers against dark background is an SEM micrograph of the same field. All images collected at nominal 20,000× magnification, with fibrous structures approximately 5 μm long

leading to negative bias. Films derived from 25+% etching have so much depth to their texture that they become almost "elastic" and can "bounce" in and out of the TEM's focal plane. We have determined that a reasonable etching for analysis of airborne fibers is between 5% and 10% — deep enough to expose subsurface fibers yet light enough to minimize textural development and visual interference. Empirically, the texture at this etching percentage appears similar to the texture of an orange's skin.

PC Filters

Preparation of PC filters is straightforward because collected fibers are retained on a flat, featureless surface Figure 1, panel a. Particles larger than the pore size will simply be collected on the surface. A carbon coat is applied directly to the filter surface, and the PC is dissolved to leave the fibers suspended in the carbon film. Two factors have greatly limited the use of PC filters for collection of asbestos from the environment. The first was the problem with asbestos contamination that was common to some PC filter batches in the 1980s.[13] This contamination seems to have declined since then, and ASTM Committee D22.07 is planning to investigate the extent of this reduction. Chatfield[14] describes a method for using hydrofluoric acid to remove any remaining contamination.

Second, PC filters are notorious for their propensity to cross-link from the heat of carbon evaporation and thus become resistant to dissolution in standard solvents, such as chloroform. Chatfield[14] has developed a solution (2 mL 99% 1-2-diaminoethane ($H_2NCH_2CH_2NH_2$) in 8 mL 1-methyl-2-pyrrolidinone (C_5H_9NO)) that will dissolve even stubbornly cross-linked PC filters in less than 15 min. However, rigid safety precautions must be followed when working with this extremely hazardous mixture.

Furthermore, we have found that certain types of grids are corroded by this mixture (Table VI). Nickel, gold, titanium, and stainless-steel grids seem to work well, with the caveats that nickel grids can become magnetized and "sticky" on steel forceps, and that gold grids are expensive and are easily bent due to their thinness and malleability. Copper alloy and molybdenum grids did not fare well during our use of the solvent as indicated in Figure 11 where grid bars not covered by carbon film were eroded. Consequently, analysts should experiment with various TEM grids to find one that will survive in their laboratory.

TABLE VI. Durability of TEM Grids in Ethylenediamine PC Solvent

Grid Composition	Brands Assessed	Durability
Gold	1	Good
Titanium	1	Good
Stainless steel	1	Good
Nickel	5	Good
Copper	8	Varies
Copper alloy	2	Poor
Molybdenum	1	Poor

Notes: TEM = transmission electron microscopy; PC = polycarbonate.

TABLE VII. Interlaboratory Variation in ELAP PT Testing for Airborne Asbestos by TEM

Asbestos Type	Generation Source	RSD
All	Aerosol	0.28
All	Aqueous	0.44
Amphibole	Aerosol	0.26
Amphibole	Aqueous	0.47
Chrysotile	Aerosol	0.33
Chrysotile	Aqueous	0.44

Notes: Relative standard deviation (RSD) is the average of RSDs for all rounds in an Asbestos/Generation category. ELAP = Environmental Laboratory Approval Program; PT = proficiency testing.

Carbon Coating

Applied carbon films must be thin enough to minimize interference with detection of thin fibrils, production of electron-diffraction patterns, and emissions of low-energy X-ray photons. At the same time, the film must be thick enough to maintain planar integrity across the TEM grid openings. The geometry of the filter surface in relation to the evaporating carbon source affects the integrity of the carbon film. In an earlier article,[15] we demonstrated that an off-rotation-axis carbon source applied to a rotating and tilting filter surface produced carbon films with the best integrity.

Aqueous versus Aerosol Generation

Once we realized that etching depth affected recovery of water-deposited fibers from MCE filters, we designed and fabricated an aerosol generator that holds 109 industry-standard 25-mm cassettes, each of which filters aerosol-laden air at 1 L/min. Aerosols were typically generated via fluidized bed that contained a mixture of asbestos in bronze pellets.[16] In our earlier PT program for airborne asbestos, we had deposited asbestos onto 0.45-μm MCE filters using aqueous suspension because aerosols seemed more likely to produce nonuniform deposition due to electrostatic interactions.

However, results from laboratories (approximately 25–30 per round) participating in the aerosol-generation ELAP PT have shown improved interlaboratory precision over earlier aqueous-generated PT samples (Table VII). The poorer precision from aqueous filtrations could be due to the widely varying etching practices among participating laboratories. The impact of aerosol vs. aqueous deposition of asbestos on PC filters was not investigated, as PC filters are not commonly used for routine analysis of airborne asbestos. Chatfield[1] does indicate that use of surfactants affects recovery of waterborne asbestos by PC and MCE filters.

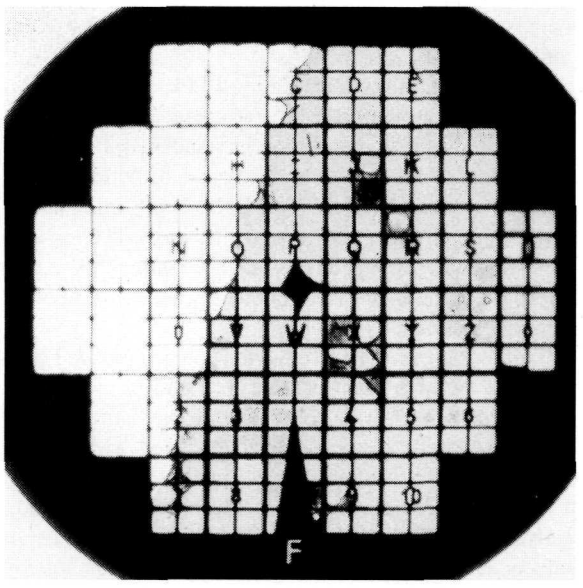

FIGURE 11. Cu-Rh TEM grid with eroded grid bars after 15-min exposure to ethylenediamine solvent

RECOMMENDATIONS

We have demonstrated that there are several filter preparation steps in common use that can bias results, but large interlaboratory variation has prevented statistical discrimination in some cases. Hence, well-designed investigations are needed to evaluate the effects of these various practices, with the goal of producing a standardized protocol that will consistently produce accurate results.

On the basis of the findings and discussion above, the following steps should improve the quality of membrane-filter preparations for asbestos analysis.

MCE filters

1. Collapse with DMF solution to avoid problems (windrows, tilted fibers) caused by HB. Use just enough DMF solution to collapse the filter (~20 μL per quarter 25-mm wedge).
2. If HB must be used,

a. dispense acetone very slowly to prevent flooding and windrows. Use of a narrow-gauge needle should reduce flooding.
b. view the entire grid at TEM low magnification to ensure that windrows have not developed
c. use an *a priori* grid-opening selection system that takes the choice out of the analyst's hands.

3. When calibrating etching rates by LTA,
   a. place in their usual orientation the number of filters typically etched in a batch.
   b. take into account mass loss due to evaporation of moisture under vacuum.
   c. aim for an etch of about 5%, which appears like orange skin.

PC Filters

1. Preparation of PC filters is straightforward, avoiding the potential variability introduced by collapsing and etching of MCE filters.
2. Use a 1, 2-diaminoethane solution to dissolve refractory filters. Be careful in its use and be prepared to try different grid alloys if the solution erodes grids being used.

Carbon Coating

Applying carbon while filter is tilting and rotating off-axis from the carbon source will improve three-dimensional coverage of particles on filter.

ACKNOWLEDGMENTS

Paul Baron, NIOSH–Cincinnati, provided substantial assistance on the design of the aerosol generator. George Matuczek of the Wadsworth Center's Instrumentation & Automation, fabricated the aerosol generator. Jon Roe, as summer student, assisted in preparation and analysis. Adrianna Verschoor improved the readability of this manuscript. Analyses were performed on electron-beam instruments in the Wadsworth Center Electron Microscopy Core, which was supported in part by an National Institutes of Health COBRE grant.

REFERENCES

1. **Chatfield, E.J.:** Measurements of chrysotile fiber retention efficiencies for polycarbonate and mixed cellulose ester filters. In *STP 1342 Advancements in Environmental Measurement Methods for Asbestos*, M.E. Beard and H.L. Rook (eds.). West Conshohocken, Pa.: American Society for Testing and Materials (2000). pp. 250–265.
2. **American Society for Standards and Materials (ASTM):** Annual Book of ASTM Standards, 2005, Vol. 11.03: Atmospheric Analysis: Occupational Health and Safety; Protective Clothing. West Conshohocken, Pa.: ASTM International, 2005. pp. 530–556, 789–819, 923–943.
3. **International Organization for Standardization (ISO):** *Ambient Air—Determination of Asbestos Fibers—Direct Transfer Transmission Electron Microscopy Method (ISO 10312:1995)* [Standard] Geneva: ISO (1995).
4. "Asbestos-Containing Materials in Schools; Final Rule and Notice," *Federal Register* 52:21 (30 October 1987). pp. 41826–41905.
5. **Chatfield, E.J., and M.J. Dillon:** *Analytical Method for Determination of Asbestos Fibers in Water* (EPA-600/4-83-043). Athens, Ga.: U.S. Environmental Protection Agency (1983).
6. **Brackett, K.A., P.J. Clark, and J.R. Millette:** *Method 100.2: Determination of Asbestos Structures Over 10 μm in Length in Drinking Water* (EPA/600R-94/134). Washington, D.C.: U.S. Environmental Protection Agency (1994).
7. **National Institute for Occupational Safety and Health (NIOSH):** *Method 7402, Asbestos by TEM*. Cincinnati, Ohio: U.S. Department of Health and Human Services, Public Health Service, Centers for Disease Control, National Institute for Occupational Safety and Health, (1994).
8. **Burdett, G., and A.P. Rood:** Membrane-filter, direct-transfer technique for the analysis of asbestos fibers or other inorganic particles by transmission electron microscopy. *Environ. Sci. Technol 17(11)*:643–648 (1983).
9. **National Institute for Occupational Safety and Health (NIOSH):** *Method 7400. Asbestos and Other Fibers by PCM*. Cincinnati, Ohio: U.S. Department of Health and Human Services, Public Health Service, Centers for Disease Control, National Institute for Occupational Safety and Health (1994).
10. **Burdett, G.J., G. Archenhold, A.R. Clark, and D. M. Hunter:** The use of scanning confocal microscopy to measure the penetration of asbestos into membrane filters. In *Advances in Environmental Measurement Methods for Asbestos, ASTM STP 1342*, M.E. Beard, H.L. Rook (eds.). West Conshohocken, Pa.: American Society for Testing and Materials (2000).
11. **Webber, J.S.:** A microcomputer program for the generation of random grid squares in quantitative analysis. *J. Electron Microsc. Tech.* 7:195–197 (1987).
12. **Dodson, R.F., M.A. Atkinson, and J.L. Levin:** Asbestos fiber length as related to potential pathogenicity: A critical review. *Am. J. Ind. Med. 44(3)*:291–297 (2003).
13. **Powers, T.J.:** Filter Blank Contamination in Asbestos Abatement Monitoring Procedures. Proceedings of a peer review workshop held at Cincinnati, OH on April 24–25, 1996. Environmental Protection Agency, Washington, D.C., EPA/600/9-86/025 (NTIS PB86244647). 1986.
14. **Chatfield, E.J.:** A rapid procedure for preparation of transmission electron microscopy specimens from polycarbonate filters. In *Advances in Environmental Measurement Methods for Asbestos, ASTM STP 1342*, M.E. Beard and H.L. Rook (eds.). West Conshohocken, Pa: American Society for Testing and Materials (2000).
15. **Webber, J.S., and R.J. Janulis:** Effects of evaporation configuration on carbon film integrity. [Online] *Environ. Inf. Assoc. J. Winter* :15–19 (1995). http://www.eia-usa.org/EIA_Archive_CD_/eia_archive_cd_.html (Accessed August 6, 2007).
16. **Carpenter, R.L., and K. Yekes:** Relationship between fluid bed aerosol generator operation and the aerosol produced. *Am. Ind. Hyg. Assoc. J. 41*:888–894 (1980).